Journal of Solid State Chemistry 185 (2012) 76–81

Contents lists available at SciVerse ScienceDirect

Journal of Solid State Chemistry

journal homepage: www.elsevier.com/locate/jssc

Nonstoichiometry, point defects and magnetic properties in $Sr_2FeMoO_{6-\delta}$ double perovskites

R. Kircheisen [a,b], J. Töpfer [a,*]

[a] University of Applied Sciences Jena, Dept. SciTec, Carl-Zeiss-Promenade 2, 07745 Jena, Germany
[b] Fraunhofer Institute of Ceramic Technology and Systems (IKTS), Faradaystrasse 1, 07629 Hermsdorf, Germany

ARTICLE INFO

Article history:
Received 6 May 2011
Received in revised form
17 October 2011
Accepted 29 October 2011
Available online 7 November 2011

Keywords:
Double perovskites
Nonstoichiometry
Magnetic properties

ABSTRACT

The phase stability, nonstoichiometry and point defect chemistry of polycrystalline $Sr_2FeMoO_{6-\delta}$ (SFMO) was studied by thermogravimety at 1000, 1100, and 1200 °C. Single-phase SFMO exists between $-10.2 \leq \log pO_2 \leq -13.7$ at 1200 °C. At lower oxygen partial pressure a mass loss signals reductive decomposition. At higher pO_2 a mass gain indicates oxidative decomposition into $SrMoO_4$ and $SrFeO_{3-x}$. The nonstoichiometry δ at 1000, 1100, and 1200 °C was determined as function of pO_2. SFMO is almost stoichiometric at the upper phase boundary (e.g. $\delta=0.006$ at 1200 °C and $\log pO_2=-10.2$) and becomes more defective with decreasing oxygen partial pressure (e.g. $\delta=0.085$ at 1200 °C and $\log pO_2=-13.5$). Oxygen vacancies are shown to represent majority defects. From the temperature dependence of the oxygen vacancy concentration the defect formation enthalpy was estimated ($\Delta H_{OV}=253\pm8$ kJ/mol). Samples of different nonstoichiometry δ were prepared by quenching from 1200 °C at various pO_2. An increase of the unit cell volume with increasing defect concentration δ was found. The saturation magnetization is reduced with increasing nonstoichiometry δ. This demonstrates that in addition to Fe/Mo site disorder, oxygen nonstoichiometry is another source of reduced magnetization values.

1. Introduction

$Sr_2FeMoO_{6-\delta}$ (SFMO) is a spin-polarized half-metal with a Curie temperature of about 410 K which exhibits large values of low-field magneto-resistance (LFMR) at room temperature [1]. These properties qualify SFMO as a promising candidate material for spintronics and sensor applications. The crystal structure of SFMO is that of a *B*-site ordered double perovskite $A_2B'B''O_{6-\delta}$ with an ordered arrangement of Fe and Mo on the perovskite *B*-sites. However, in reality ideal ordering of *B* and *B*′ cations is not reached and some degree of antisite disorder (ASD), i.e. Fe on Mo sites and vice versa, is observed [2]. At room temperature SFMO crystallizes in a tetragonal unit cell; the space group $I4/mmm$ was suggested by many authors, e.g. [2]. At around 400 K a phase transition to a cubic $Fm\bar{3}m$ structure occurs [3]. However, the space group of the room temperature tetragonal structure has been debated for quite a while. Neutron diffraction measurements seem to indicate that $I4/m$ most likely is the correct space group [3,4]. The magnetism of SFMO is discussed as being due to antiferromagnetic interactions between the localized Fe^{3+} ions ($t_{2g}^3\,e_g^2$, $S=5/2$) and itinerant $4d^1$ Mo^{5+} ions (e_g^1, $S=½$) resulting in a ferrimagnetic arrangement with a saturation magnetization of 4 μ_B [1,2]. Mössbauer [5] and NMR [6] spectroscopy have revealed a partial transfer of electron density resulting in a mixed valence situation with high-spin $Fe^{2.5+}$ ($3d^{5.5}$) and $Mo^{5.5+}$ ($4d^{0.5}$) giving rise to the same value of M_s. The magnetization was shown to be sensitive to the degree of cation ordering. A correlation between preparation temperature, cationic disorder and magnetization was shown by Balcells et al. [2]. The kinetics of the ordering process was monitored by Shimada et al. [7], and maximum ordering could be achieved at prolonged sintering at around 1150 °C. Samples with a very high degree of cation order were prepared through a complex gel route and sintering in silica ampoules with a Fe getter; this synthesis procedure results in a maximum M_s of 3.96 μ_B [8]. It was demonstrated, that the magnitude of the LFMR also depends on the degree of ASD [9]. Disordered intergrowths were detected as another source of reduced M_s and MR [10]. Moreover, it was shown that oxygenation/reduction treatments can reversibly change the oxygen stoichiometry and grain boundary composition and, hence, MR properties [11]. Another model has been put forward recently that allows to interpret the observed variation of the electronic and magnetic properties with the degree of cation ordering as a signature of a polaronic–itinerant electronic transition with well-ordered itinerant regions growing in a partially ordered matrix phase [12].

* Corresponding author. Fax: +49 3641 205451.
E-mail address: joerg.toepfer@fh-jena.de (J. Töpfer).

0022-4596/$ - see front matter © 2011 Elsevier Inc. All rights reserved.
doi:10.1016/j.jssc.2011.10.043

$Sr_2FeMoO_{6-\delta}$ is commonly prepared through calcinations of the starting oxides in air and sintering under reducing gas atmosphere (Ar/H_2 mixtures). However, precise knowledge about the boundaries of the SFMO phase field is limited. Many studies reported in the literature are performed on samples containing different amounts of impurity phases. Moreover, precise experimental sintering conditions, i.e. the oxygen partial pressure, are not reported in most of the papers. Nakamura et al. [13] have shown in an early study that SFMO exists at 1200 °C in a limited stability range only at low pO_2. The phase relations of the system $SrO–Fe_3O_4–MoO_3$ at 1200 °C in $Ar/1\%H_2$ were investigated [14]. Information on the oxygen stoichiometry δ of $Sr_2FeMoO_{6-\delta}$ are scarce. Rager et al. [14] report δ-values determined by a hot extraction method; for SFMO sintered at 1200 °C in $Ar/1\%H_2$ they found $\delta=0.2$. Yamamoto et al. measured $\delta=0.03$ using a coulometric titration technique for a sample synthesized at 1150 °C in an evacuated silica ampoule with Fe getter and $pO_2=2.6\times10^{-13}$ atm [15]. Chang et al. [16] report on a large nonstoichiometry of $\delta=0.16$ for sintered samples which were annealed at 850 °C in a $N_2/5\%H_2$ atmosphere. Nonstoichiometry data of SFMO are conflicting. To the best of our knowledge, no systematic study on the variation of δ in $Sr_2FeMoO_{6-\delta}$ with T or pO_2 has been performed yet. On the other hand, it is expected that the nonstoichiometry has a distinct effect on the magnetic and magneto-resistive properties as well. It was pointed out, that oxygen vacancies might reduce the magnetization significantly [17]. In a very recent theoretical study using density functional theory calculations it was shown that cation antisites and oxygen vacancies are the dominating phenomena that reduce the magnetization [18].

We have already demonstrated in a preliminary study that the nonstoichiometry δ of SFMO at 1200 °C varies as a function of pO_2 and can be modeled based on oxygen vacancies as majority point defects [19]. It was shown that samples with small δ display large saturation magnetizations, whereas a larger nonstoichiometry results in reduced M_s and large magneto-resistance at room temperature. In this paper we present results of the measurement of the nonstoichiometry δ of $Sr_2FeMoO_{6-\delta}$ at 1000, 1100, and 1200 °C. Structural and magnetic properties of samples with different nonstoichiometries δ are discussed.

2. Experimental

SFMO samples were prepared with a standard mixed-oxide route starting from $SrCO_3$, MoO_3, and Fe_2O_3. The raw materials were homogenized in isopropanol. After calcination at 900 °C in air, the powders were milled in isopropanol. After compaction the pellets were sintered at 1200 °C for 20 h in an $Ar/2\%H_2$ atmosphere. Measurements of the nonstoichiometry δ were performed in a Setaram thermobalance TGA92 at 1000, 11000, and 1200 °C and different partial pressures of oxygen. Gas atmospheres were established with $N_2/CO/CO_2$ mixtures and the pO_2 was measured with zirconia oxygen sensors at the inlet/outlet positions of the gas mixture into/out of the balance system. In a typical run, the sample was held at the reference oxygen partial pressure (e.g. $\log pO_2=-11.84$ at 1200 °C) until equilibrium was reached as signaled by a constant mass. Then the pO_2 was changed to another value and the corresponding mass change recorded. After equilibrium was reached (typically several hours), the pO_2 was switched back to the reference pO_2 to check the process reversibility. The measured mass changes were transformed into changes of nonstoichiometry, $\Delta\delta$, using the relation $\Delta\delta=(\Delta m M_{SFMO})/(m_0 M_o)$ with m_0 as the initial sample mass and M as the molar mass of SFMO and oxygen. Absolute values of the nonstoichiometry δ were obtained by fitting the data to the equation

$$\Delta\delta=\delta-\delta_0=kp_{O_2}^{n}-\delta_0 \quad (1)$$

with the nonstoichiometry at the reference oxygen partial pressure δ_0. The parameters δ_0, k, and n were determined and values of δ were calculated.

Samples with different values of the nonstoichiometry δ were prepared by annealing the sintered pellets in the thermobalance. The pellets were held at 1200 °C and the reference oxygen partial pressure until a constant mass indicates that equilibrium is established (typically 10 h). Then, the oxygen partial pressure was changed to another value corresponding to the desired nonstoichiometry δ and the sample was held there for about 24 h for complete equlibriation. Finally, the samples were rapidly cooled in the balance with a rate of 35 K/min.

Powder X-ray diffraction measurements (XRD) were performed with a Siemens D5000 using Cu$K\alpha$ radiation (step time 8 s; step size 0.02°; 10–75° 2θ). Lattice parameters and antisite concentrations were refined using the TOPAS R software package (Bruker AXS, Karlsruhe, Germany). The antisite defect concentration (AS per formula unit) was determined by refining the occupation of Fe and Mo positions; the concentration of antisites per f.u. corresponds to the number of misplaced Fe or Mo ions (i.e. zero for perfect order and 0.5 for complete disorder).

Magnetic properties were measured with a Quantum Design SQUID magnetometer. Hysteresis loops M(H) were measured at 5 K. The magnetization at the maximum field of 50 kOe was taken as saturation magnetization M_s.

3. Results and discussion

3.1. Phase stability

$Sr_2FeMoO_{6-\delta}$ is stable at low oxygen partial pressures only and becomes unstable under more oxidizing or reducing conditions, respectively. We have determined the location of the upper and lower phase boundaries of SFMO at 1200 °C by thermogravimetry (TG) and XRD. The TG analysis for the characterization of SFMO at 1200 °C in the vicinity of the upper phase boundary is shown in Fig. 1. The sample was held at a reference oxygen partial pressure ($\log pO_2=-11.8$) until equilibrium was reached as signaled by constant mass. Then the pO_2 was increased stepwise (and decrease back to the reference pO_2) as demonstrated in

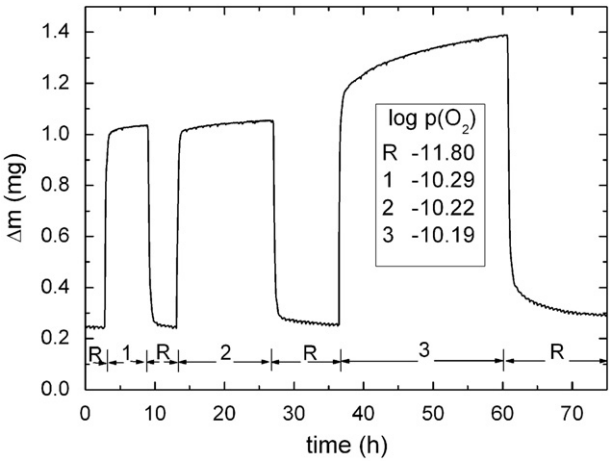

Fig. 1. Variation of the sample mass of $Sr_2FeMoO_{6-\delta}$ with time at 1200 °C for three consecutive oxidation steps induced by jumps of the oxygen partial pressure; R as reference pO_2, the oxygen partial pressures 1 and 2 are within the SFMO stability field, whereas 3 is above the upper phase boundary.

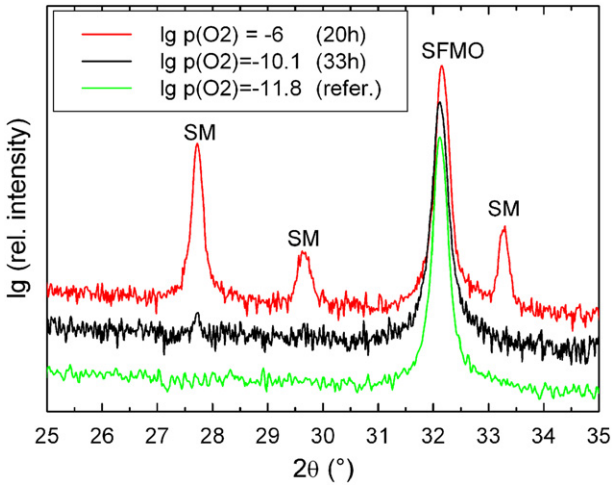

Fig. 2. Part of the X-ray diffraction patterns of SFMO samples quenched from 1200 °C and different oxygen partial pressures: $\log pO_2 = -11.8$ as reference pO_2 with single phase SFMO (bottom), $\log pO_2 = -10.1$ (middle), and $\log pO_2 = -6.0$ (top) above the upper phase boundary with formation of $SrMoO_4$ (SM).

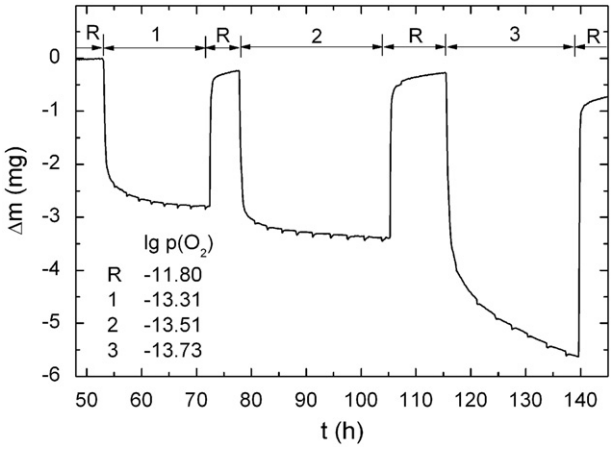

Fig. 3. Variation of the sample mass of $Sr_2FeMoO_{6-\delta}$ with time at 1200 °C for three consecutive reduction steps induced by jumps of the oxygen partial pressure; *R* as reference pO_2, the oxygen partial pressures 1 and 2 are within the SFMO stability field, whereas 3 is below the lower phase boundary.

Fig. 1. As long as the sample is at pO_2 within the SFMO field, the sample mass became constant after several hours indicating that the corresponding nonstoichiometry δ has been established (shown here for $\log pO_2 = -10.29$ and -11.22, respectively, in Fig. 1). In contrast to that, at slightly higher oxygen partial pressure ($\log pO_2 = -10.19$) the sample mass continuously increased for a holding time of more than 20 h and did not approach equilibrium. This indicates that the sample is outside the SFMO stability field under these conditions and that decomposition of SFMO proceeds. Consequently, the location of the upper phase boundary at 1200 °C is at $\log pO_2 = -10.20$. At larger oxygen partial pressures SFMO is oxidized according to:

$$Sr_2FeMoO_6 + 1/4O_2 \rightleftarrows SrMoO_4 + SrFeO_{2.5} \quad (2)$$

The location of the upper phase boundary was confirmed by XRD measurements on quenched samples (Fig. 2). For example, a sample quenched from $\log pO_2 = -11.8$ proved single-phase to XRD, whereas a sample quenched from $\log pO_2 = -10.1$ exhibits weak reflections of $SrMoO_4$, signaling the beginning of SFMO decomposition. In Fig. 2 the (112) main peak of $SrMoO_4$ at $2\theta = 27.6°$ appears with low intensity in this sample. Another sample annealed at more oxidizing conditions of $\log pO_2 = -6$ clearly exhibits reflections of $SrMoO_4$ and $SrFeO_{2.5}$ (not shown in Fig. 2).

The location of the upper phase boundary at 1200 °C is in fair agreement with the value of $\log pO_2 = -9.8$ as reported by Nakamura et al. [13] and slightly higher compared to the upper phase stability limit at $\log pO_2 = -10.65$ measured by Sharma et al. by coulometric titration [20].

The location of the lower phase boundary at 1200 °C was determined by similar TG experiments (Fig. 3). It is shown that for $\log pO_2 = -13.31$ and -13.51 equilibrium within the SFMO phase field is reached. At $\log pO_2 = -13.73$ a much larger mass loss indicates that the sample is reduced and equilibrium is not reached after 20 h. Therefore the lower phase stability limit of SFMO is in between $\log pO_2 = -13.51$ and -13.73. This is in good agreement with the only other value of $\log pO_2 = -13.5$ from the literature [13]. This is verified by XRD of a sample quenched from $T = 1200$ °C and $\log pO_2 = -14.15$ (Fig. 4). The diffractogram of that sample clearly shows partial decomposition of SFMO and formation of Sr_3FeMoO_7 and Fe.

The phase boundaries at 1100 and 1000 °C were not precisely determined. However, the pO_2 values used for the measurement of the SFMO nonstoichiometry (see next chapter) are clearly within the SFMO phase fields at both temperatures too.

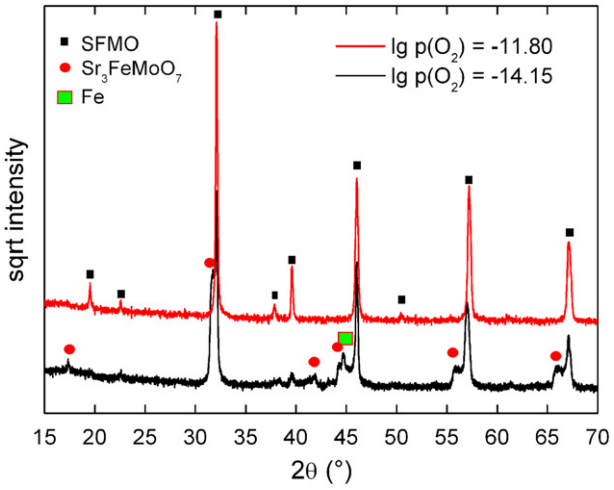

Fig. 4. Part of the X-ray diffraction patterns of SFMO samples quenched from 1200 °C and different oxygen partial pressures: $\log pO_2 = -11.8$ as reference pO_2 with single phase SFMO (top), and $\log pO_2 = -14.15$ below the lower phase boundary with formation of Sr_3FeMoO_7 and Fe (bottom).

3.2. Nonstoichiometry and point defects

The variation of the nonstoichiometry δ vs. pO_2 at 1000, 1100, and 1200 °C is shown in Fig. 5. At 1200 °C SFMO exhibits a small nonstoichiometry of $\delta = 0.006$ close to the upper phase boundary at $\log pO_2 = -10.2$. At 1100 and 1000 °C the nonstoichiometry at higher oxygen partial pressures is smaller, i.e. SFMO is almost stoichiometric in the vicinity of the upper phase boundary. At lower oxygen partial pressures larger deviations from stoichiometry are observed; e.g. $\delta = 0.085$ at 1200 °C close to lower phase boundary at $\log pO_2 = -13.5$. The nonstoichiometry values of SFMO reported here agree well with the singular value of $\delta = 0.03$ at 1150 °C and $\log pO_2 = -12.58$ reported by Yamamoto et al. [15]. However, the large nonstoichiometry of $\delta = 0.2$ reported for a sample prepared at 1200 °C in Ar/1%H_2 [14] is too large and outside the range of δ-values determined in the present study.

The nonstoichiometry δ in $Sr_2FeMoO_{6-\delta}$ can be accommodated as oxygen vacancies:

$$O_O^x \rightleftarrows V_O^{\bullet\bullet} + 2e' + 1/2O_2 \quad (3)$$

From the law of mass action and the electroneutrality condition $2[V_O^{\bullet\bullet}] = [e']$ the variation of δ as a function of pO_2 for oxygen vacancies formation is derived as $\delta = [V_O^{\bullet\bullet}] \sim p_{O_2}^{-1/2}$. Evaluation of the nonstoichiometry data within the SFMO stability range according to Eq. (1) results in $k = -(1.4 \pm 0.4) \times 10^{-6}$ and $n = -0.35 \pm 0.01$ for $T = 1200\,^{\circ}C$, $k = -(2.0 \pm 1.3) \times 10^{-7}$ and $n = -0.37 \pm 0.02$ for $T = 1100\,^{\circ}C$, and $k = -(6.5 \pm 1.3) \times 10^{-8}$ and $n = -0.35 \pm 0.01$ for $T = 1000\,^{\circ}C$, respectively. The estimated values of the exponent n significantly deviate from the expected value of $n = -0.5$. This demonstrates that the simple picture of the formation of isolated oxygen vacancies as majority point defects is a crude approximation only. This discrepancy might be due to interactions at lower pO_2 between oxygen vacancies and surrounding cations to form defect associates.

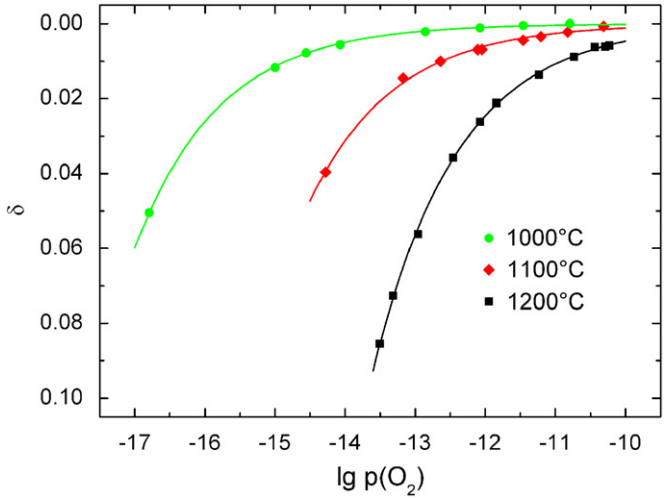

Fig. 5. Nonstoichiometry δ of $Sr_2FeMoO_{6-\delta}$ as function of oxygen partial pressure at 1000, 1100, and 1200 °C; lines are fits to Eq. (1).

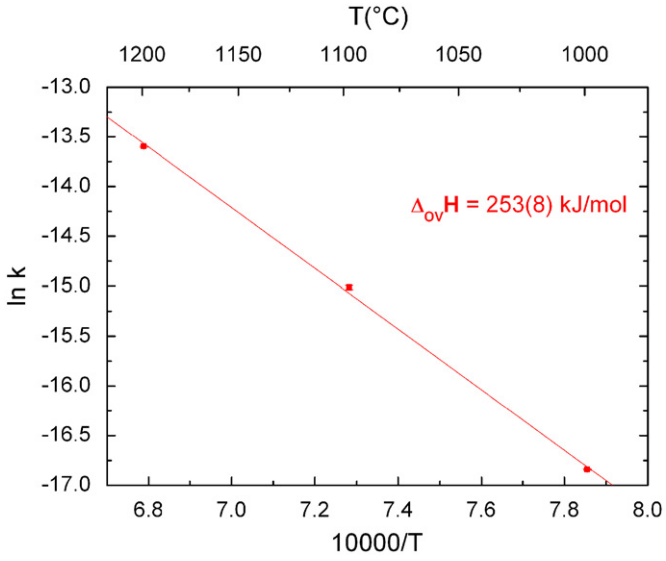

Fig. 6. Variation of ln k vs. the inverse temperature.

Since the parameter k in Eq. (1) has the dimension of an equilibrium constant, one can extract the defect formation enthalpy from the temperature dependence of k (Fig. 6). We have estimated the defect enthalpy based on values of k resulting from fits of the δ vs. pO_2 curves with the mean value of $n = -0.36 \pm 0.01$. The resulting enthalpy for the formation of oxygen vacancies in SFMO is $\Delta_{ov}H = (253 \pm 8)$ kJ/mol. This value is similar to the oxygen vacancy formation enthalpy $\Delta_{ov}H = (349 \pm 6)$ kJ/mol of $LaMnO_{3-\delta}$ in the low oxygen partial pressure regime [21]. The oxygen vacancy formation in $SrFeO_{3-\delta}$ has an enthalpy of $\Delta_{ov}H = 80$ kJ/mol only [22] and, hence, a much larger range of nonstoichiometry.

3.3. Structure and magnetism of nonstoichiometric samples

To study the influence of nonstoichiometry δ on the magnetic properties of SFMO, we prepared a set of eight samples at 1200 °C and different pO_2. The preparation conditions, corresponding nonstoichiometry values δ and lattice parameters are given in Table 1. XRD showed all samples to be single phase double perovskites, no reflections of secondary phases were detected (Fig. 7). The unit cell parameters, as determined from Rietveld refinements of the diffractograms in space group $I4/m$, are shown as function of δ in Fig. 8a. The lattice parameter a_0 increases, whereas c_0 slightly decreases with increasing defect concentration δ. The unit cell parameters are in good agreement with those reported for an almost stoichiometric sample [23], or those reported by Vasala et al. for a sample with $\delta \approx 0.04$ [24] (although the data were refined in a triclinic space group I-1). However, the unit cell volume expands with increasing δ (Fig. 8b). This is due to the formation of lower valence cations as result of charge compensation. The relative intensity of the (101) reflection as function of the defect concentration δ is shown in Fig. 9. The intensity of this superstructure peak is an indication of the degree of ordering of Fe and Mo cations within the unit cell. Balcells et al. [2] defined the ratio $I_{101}/(I_{200}+I_{112})$ as semi-quantitative order parameter. For our samples the intensity ratio exhibits a slight decrease with increasing δ. This is attributed to a modest increase of disorder connected with the formation of oxygen vacancies. Accordingly, the concentration of antisite defects (as determined from Rietveld refinements) increases with δ (Fig. 9).

Table 1
Preparation conditions (1200 °C, pO_2), lattice parameters, superstructure peak intensity ratios, Fe occupations on Fe position, antisite concentration per formula unit, and saturation magnetizations of $Sr_2FeMoO_{6-\delta}$ samples.

No.	log pO_2	δ	a_0 (Å)	c_0 (Å)	Vol. (Å^3)	$I_{101}/(I_{200}+I_{112})$	Fe occ	AS per f.u.	M_s (μ_B)
1	−10.12	0.0055	5.5704(1)	7.9028(2)	245.22(1)	0.0570	0.935(4)	0.065(4)	3.57
2	−10.48	0.0073	5.5709(1)	7.9032(2)	245.28(1)	0.0414	0.940(4)	0.060(4)	3.36
3	−11.66	0.0191	5.5711(1)	7.9023(2)	245.27(1)	0.0332	0.927(4)	0.073(4)	3.31
4	−12.48	0.0373	5.5728(3)	7.8989(6)	245.31(3)	0.0381	0.925(5)	0.075(5)	3.43
5	−12.91	0.0529	5.5732(1)	7.8997(2)	245.37(1)	0.0360	–	–	–
6	−12.98	0.0560	5.5745(2)	7.8955(7)	245.35(3)	0.0257	0.889(5)	0.111(5)	3.22
7	−13.07	0.0603	5.5733(1)	7.9001(2)	245.38(1)	0.0319	0.905(5)	0.095(5)	3.30
8	−13.58	0.0913	5.5764(2)	7.8925(3)	245.43(3)	0.0307	0.888(4)	0.112(4)	3.13

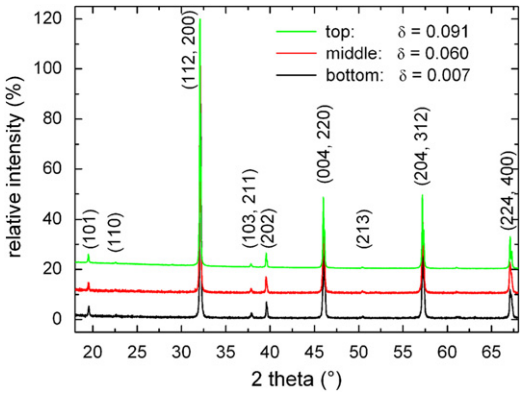

Fig. 7. X-ray diffraction patterns of single phase SFMO samples prepared at 1200 °C and log $pO_2 = -10.48$ with $\delta = 0.007$ (bottom), at log $pO_2 = -13.07$ with $\delta = 0.060$ (middle), and at log $pO_2 = -13.58$ with $\delta = 0.091$ (top).

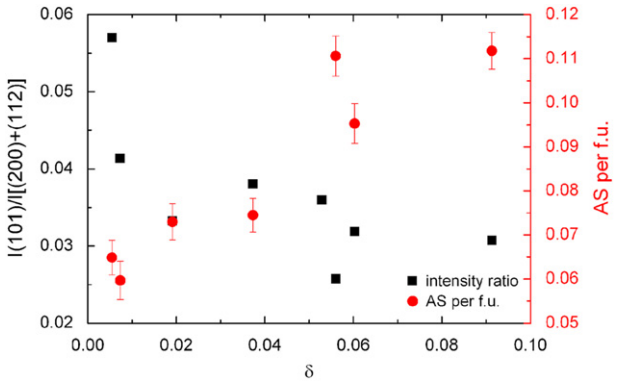

Fig. 9. Intensity ratio of XRD reflections (110)/[(200)+(112)] and refined antisite concentration (AS per formula unit) as function of nonstoichiometry δ for $Sr_2FeMoO_{6-\delta}$.

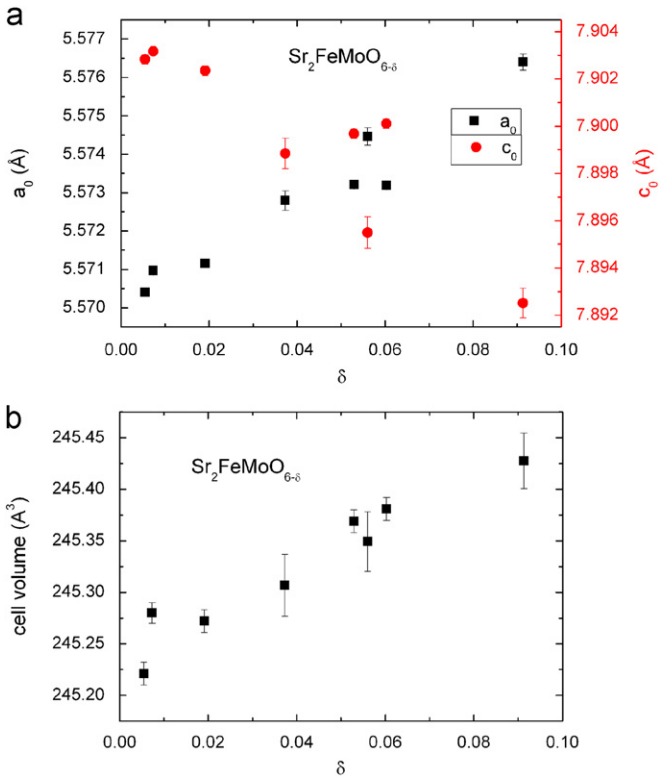

Fig. 8. Unit cell parameters (a) and volume (b) as function of nonstoichiometry δ for $Sr_2FeMoO_{6-\delta}$.

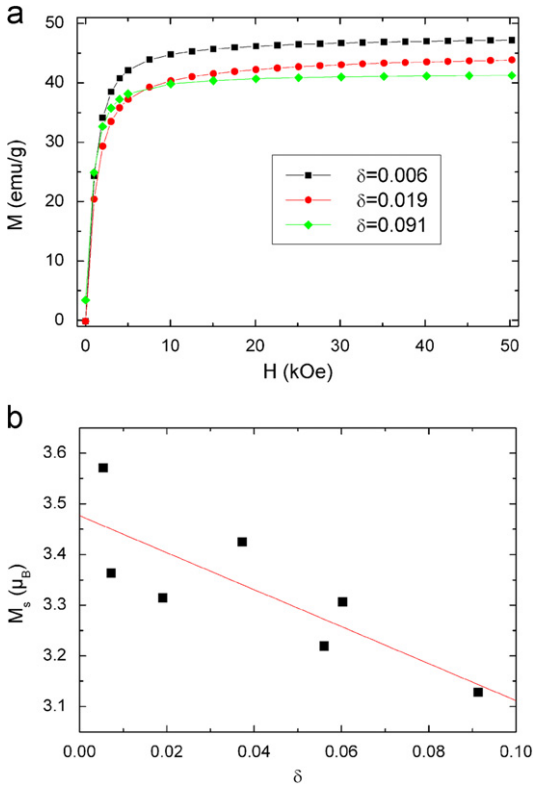

Fig. 10. Magnetization vs. field at $T = 5$ K (a) for SFMO samples prepared at 1200 °C and log $pO_2 = -10.12$ with $\delta = 0.006$ (top), at log $pO_2 = -11.66$ with $\delta = 0.019$ (middle), and at log $pO_2 = -13.58$ with $\delta = 0.091$ (bottom), and saturation magnetization M_s at $T = 5$ K as function of nonstoichiometry δ for $Sr_2FeMoO_{6-\delta}$ (b).

The magnetization measured as a function of the magnetic field ($T = 5$ K) is saturated at a field of 50 kOe (Fig. 10a). Saturation magnetizations (Fig. 10b) were found to be maximum (3.6 μ_B) for an almost stoichiometric sample. Increasing oxygen vacancy concentrations tend to reduce M_s. Saturation magnetizations smaller than 4 μ_B were reported in many other studies. Usually, samples are prepared in Ar/H_2 gas mixtures; if the hydrogen concentration in the gas mixture is large ($>1\%$) this causes extensive oxygen vacancy formation or even partial sample decomposition. Balcells et al. [2] and many others have shown that the synthesis temperature is an important factor that influences cation ordering and, hence, the saturation magnetization. A strong correlation between the antisite defect concentration and M_s was found. The magnetization is reduced at a rate of $M_s = 4\ \mu_B - 8$/ASD concentration. A maximum $M_s = 3.7\ \mu_B$ was measured for a well ordered sample [2]. It was demonstrated that the use of reactive precursors and prolonged heating at intermediate temperatures improves the cation ordering and, hence, the magnetization; maximum M_s values of almost 4 μ_B were reported [7,8]. Another model that focuses on the partial decomposition of SFMO upon oxygenation (change of the 1:1 Fe/Mo ratio and formation of grain boundary phases) was proposed to explain reduced M_s values [11]. In this study we show, that the pO_2 of the surrounding gas atmosphere is another important parameter, since the formation of oxygen vacancies leads to the formation of lower valence cations (e.g. formation of ferrous ions with $S = 4/2$, or Mo^{4+} with $S = 1$), thus reducing M_s. This situation results in a reduction of M_s with a rate of $4\ \mu_B - 2\delta$. This model

was recently proposed based on ab-initio calculations [17]. The magnetization data in Fig. 10b indicate that M_s is reduced from $M_s=3.5\ \mu_B$ at $\delta=0$ to $M_s=3.1\ \mu_B$ at $\delta=0.1$ (linear fit in Fig. 10b). The fact that the nearly stoichiometric samples already exhibit a reduced magnetization of $<4\ \mu_B$ is attributed to the presence of a certain level of antisite disorder in these samples. Hence the magnetization reduction due to defect formation now is defined by $3.5\ \mu_B-2\delta$. If the reduction of M_s would be due to oxygen vacancies only, a $M_s=3.3$ would be expected for $\delta=0.1$, but the observed reduction of M_s is somewhat larger than the predicted rate of $-2/\delta$. This might be explained by the simultaneous increase of the cation antisite disorder (ASD) with increasing concentration of oxygen vacancies δ, as shown in Fig. 9. However, it is demonstrated that nonstoichiometry and the formation of oxygen vacancies is another source for reduced magnetization values.

4. Conclusions

The double perovskite $Sr_2FeMoO_{6-\delta}$ (SFMO) is stable only at low oxygen partial pressure, e.g. between $-10.2\le\log pO_2\le-13.7$ at 1200 °C. SFMO exhibits a significant nonstoichiometry δ as measured by thermogravimety at 1000, 1100, and 1200 °C. At higher pO_2 close to the upper phase boundary SFMO is almost stoichiometric (e.g. $\delta=0.006$ at 1200 °C and $\log pO_2=-10.2$), but δ increases with decreasing oxygen partial pressure (e.g. $\delta=0.085$ at 1200 °C and $\log pO_2=-13.5$). The nonstoichiometry is accommodated by oxygen vacancies. The defect formation enthalpy is $\Delta H_{OV}=253\pm8$ kJ/mol. The oxygen vacancies might be associated to form clusters; this requires further investigations.

The unit cell volume and the antisite concentration of nonstoichiometric SFMO increases with increasing oxygen vacancy concentrations. The saturation magnetization decreases with δ. This demonstrates that in addition to Fe/Mo antisite disorder oxygen nonstoichiometry δ is another source of reduced magnetization values.

Acknowledgments

The authors thank S. Barth (IKTS Hermsdorf, Germany) for the preparation of the starting SFMO material. Financial support by the Bundesministerium für Bildung und Forschung (Germany) is acknowledged (Grant 03WKF22E).

References

[1] K.I. Kobayashi, T. Kimura, H. Sawada, K. Terakura, Y. Tokura, Nature 395 (1998) 677.
[2] L. Balcells, J. Navarro, M. Bibes, A. Roig, B. Martinez, J. Fontcuberta, Appl. Phys. Lett. 78 (3) (2001) 781.
[3] O. Chmaissem, R. Kruk, B. Dabrowski, D.E. Brown, X. Xiong, S. Kolesnik, J.D. Jorgensen, C.W. Kimball, Phys. Rev. B 62 (2000) 14197 #.
[4] S. Nakamura, K. Oikawa, J. Phys. Soc. Jpn. 72 (12) (2003) 3123–3127.
[5] J. Linden, T. Yamamoto, M. Karppinen, H. Yamauchi, Appl. Phys. Lett. 76 (2000) 2925.
[6] C. Kapusta, P.C. Riedi, D. Zajac, M. Sikora, J.M. De Teresa, L. Morellon, M.R. Ibarra, J. Magn. Magn. Mater. 242–245 (2002) 242–245.
[7] T. Shimada, J. Nakamura, T. Motohashi, H. Yamauchi, M. Karpinnen, Chem. Mater. 15 (2003) 4494.
[8] Y.H. Huang, J. Linden, H. Yamauchi, M. Karppinen, Chem. Mater. 16 (2004) 4337–4342.
[9] M. Garcia-Hernandez, J.L. Martinez, M.J. Martinez-Lope, M.T. Casais, J.A. Alonso, Phys. Rev. Lett. 86 (2001) 2443.
[10] X.Z. Liao, A. Sharma, M. Wei, J.L. MacManus-Driscoll, W. Branford, L. Cohen, Y. Bugoslavsky, Y.T. Zhu, D. Peterson, Y. Jiang, H. Xu, J. Appl. Phys. 96 (2004) 7747.
[11] J. MacManus-Driscoll, A. Sharma, Y. Bugoslavsky, W. Branford, L.F. Cohen, M. Wei, Adv. Mater. 18 (2006) 900.
[12] Y.H. Huang, M. Karppinen, H. Yamauchi, J.B. Goodenough, Phys. Rev. B 73 (2006) 104408.
[13] T. Nakamura, K. Kunihara, Y. Hirose, Mat. Res. Bull. 16 (1981) 321.
[14] J. Rager, M. Zipperle, A. Sharma, J.L. MacManus-Driscoll, J. Am. Ceram. Soc. 87 (2004) 1330.
[15] T. Yamamoto, J. Liimatainen, J. Linden, M. Karppinen, H. Yamauchi, J. Mater. Chem. 10 (2000) 2342–2345.
[16] H. Chang, M. Garcia-Hernandez, J.A. Alonso, Appl. Phys. Lett. 89 (2006) 182501.
[17] S. Collis, D. Stoeffler, C. Meny, T. Fix, C. Leuvrey, G. Pourroy, A. Dinia, P. Panissod, J. Appl. Phys. 98 (2005) 033905.
[18] R. Mishra, O.D. Restrepo, P.M. Woodward, W. Windl, Chem. Mater. 22 (2010) 6092–6102.
[19] J. Töpfer, R. Kircheisen, S. Barth, J. Appl. Phys. 105 (2009) 07D712.
[20] A. Sharma, J.L. MacManus-Driscoll, W. Branford, Y. Bugoslavsky, L.F. Cohen, J. Rager, Appl. Phys. Lett. 87 (2005) 112505.
[21] J.A.M. van Rossmalen, E.H.P. Cordfunke, J. Solid Stae. Chem 110 (1994) 113–117.
[22] A. Holt, T. Norby, R. Glenne, Ionics 5 (1999) 434–443.
[23] D. Niebieskikwiat, A. Caneiro, R.D. Sanchez, J. Fontcuberta, Phys. Rev. B 64 (2001) 180406.
[24] S. Vasala, M. Lehtimäki, Y.H. Huang, H. Yamauchi, J.B. Goodenough, M. Karppinen, J. Solid State Chem. 183 (2010) 1007–1012.